Modulation of Primary Radical Pair Kinetics and Energetics in Photosystem II by the Redox State of the Quinone Electron Acceptor Q_A

Krzysztof Gibasiewicz,*† Andrzej Dobek,† Jacques Breton,* and Winfried Leibl*
*Section de Bioénergétique, DBCM, F-91191 Gif-sur-Yvette Cedex, France; and †Institute of Physics, Adam Mickiewicz University, 61–614 Poznan, Poland

ABSTRACT Time-resolved photovoltage measurements on destacked photosystem II membranes from spinach with the primary quinone electron acceptor Q_A either singly or doubly reduced have been performed to monitor the time evolution of the primary radical pair $P680^+Pheo^-$. The maximum transient concentration of the primary radical pair is about five times larger and its decay is about seven times slower with doubly reduced compared with singly reduced Q_A. The possible biological significance of these differences is discussed. On the basis of a simple reversible reaction scheme, the measured apparent rate constants and relative amplitudes allow determination of sets of molecular rate constants and energetic parameters for primary reactions in the reaction centers with doubly reduced Q_A as well as with oxidized or singly reduced Q_A. The standard free energy difference $\Delta G°$ between the charge-separated state $P680^+Pheo^-$ and the equilibrated excited state $(Chl_NP680)^*$ was found to be similar when Q_A was oxidized or doubly reduced before the flash (~ -50 meV). In contrast, single reduction of Q_A led to a large change in $\Delta G°$ ($\sim +40$ meV), demonstrating the importance of electrostatic interaction between the charge on Q_A and the primary radical pair, and providing direct evidence that the doubly reduced Q_A is an electrically neutral species, i.e., is doubly protonated. A comparison of the molecular rate constants shows that the rate of charge recombination is much more sensitive to the change in $\Delta G°$ than the rate of primary charge separation.

INTRODUCTION

Photosystem II (PS II) is a membrane-bound protein complex that catalyzes the conversion of light energy into a more stable form of electrochemical energy during the primary processes of oxygenic photosynthesis (for a review see Diner and Babcock, 1996). With respect to the structure and function, the core subunits of PS II are thought to be similar to those of the better characterized purple bacterial reaction centers (RCs), both belonging to the family of quinone-type RCs (Rutherford and Nitschke, 1996). Light absorption by chlorophylls in antenna proteins (light-harvesting complexes) leads to the creation of excited singlet states, called excitons. The excitons are rapidly equilibrated within the antenna as well as between the antenna and RC (McCauley et al., 1989; Holzwarth, 1991). The excited states can be depopulated either by trapping in the RC (photochemical quenching), by internal conversion, or by emission of fluorescence (Geacintov and Breton, 1987). The trapping is defined as the conversion of an excited state into a charge-separated state in the RC. This primary charge separation occurs by electron transfer from an excited primary donor, a chlorophyll species (P680), to a primary electron acceptor, a pheophytin (Pheo), creating the primary radical pair $P680^+Pheo^-$. The primary radical pair (RP) decays by forward electron transfer to the first quinone electron acceptor Q_A ($\tau \approx 500$ ps) when the latter is oxidized (open RC), or by charge recombination in the nanosecond range when Q_A is already reduced (closed RC). This charge recombination may occur by several competing pathways such as reformation of the excited singlet state P680*, direct recombination to the ground state, or via singlet-triplet mixing to populate the triplet state of the primary donor.

PS II is generally considered as a shallow trap, with the free energy of the charge-separated state being close to the one of the excited state (van Gorkom, 1985). There are two main reasons why PS II is different from the other photosystems in that respect. First, the energy transfer between the antenna chlorophylls and the primary donor is largely reversible due to similar energy levels of their excited states Chl* and P680*. In a first approximation, full equilibration of the excited states leads to a decrease of the free energy of the state $(Chl_NP680)^*$ compared with that of Chl_NP680^*, due to an entropy term $S = k_BT \ln N^{eff}$, where N^{eff} is the effective number of pigments over which the excitation is equilibrated (see below) (Trissl, 1993; van Mieghem et al., 1995). At physiological temperatures and due to the relatively large antenna size, this entropy contribution amounts to ~ -120 meV. Second, the extremely positive redox midpoint potential of the primary donor $E_m(P680^+/P680)$, of the order of +1.1 eV, necessary to drive the oxidation of water, causes its excited singlet state redox potential $E_m(P680^*/P680^+)$ to be less negative than in all other systems. Both effects bring the free energy of the equilibrated excited state $(Chl_NP680)^*$ close to the level of the radical pair state $P680^+Pheo^-$. As a consequence, trapping has to be considered as a reversible reaction and is usually described by an exciton/radical pair equilibrium model (Schatz et al., 1988; Leibl et al., 1989).

Received for publication 29 December 1999 and in final form 27 December 2000.

Address reprint requests to Dr. Winfried Leibl, Section de Bioénergétique, CEA Saclay, 91191 Gif-sur-Yvette, France. Tel.: 33-1-6908-5289; Fax: 33-1-6908-8717; E-mail: leibl@dsvidf.cea.fr.

0006-3495/01/04/1617/14 $2.00

The formation of the primary radical pair is a crucial step of photosynthetic energy conversion as it has to be kinetically competitive with wasteful loss processes depopulating the excited states. The small driving force makes the yield of primary charge separation in PS II particularly sensitive to small changes in the energetics. A well-known example is the large increase in fluorescence yield upon reduction of Q_A. It is interpreted as a shift of the equilibrium between the charge-separated state and the equilibrated excited state toward the excited state (Schatz et al., 1988). From the kinetic point of view, equilibration of the excited state is much faster than its lifetime. Therefore, the trapping is considered as limited by the primary charge separation in the RC, i.e., trap-limited (e.g., Schatz et al., 1988; Leibl et al., 1989). The shallow-trap properties of PS II make this system interesting to study the influence of small energy changes induced by electrostatic interactions within the proteins on the kinetics of intra-protein electron transfer.

The efficiency of charge stabilization on Q_A depends to a large extent on the ratio of the rate constants for electron transfer from $Pheo^-$ forward to Q_A and backward to $P680^+$. However, the latter rate constant is not easily accessible. One approach to assess the intrinsic rate of back-reaction is to block the forward electron transfer to Q_A. In principle this can be realized by pre-reducing Q_A to Q_A^-, either by light or chemically. However, according to various authors, the single reduction of Q_A makes the primary charge separation slower and less efficient (Schatz et al., 1988; Roelofs et al., 1992) and/or makes the charge recombination faster compared with RCs with oxidized Q_A (Leibl et al., 1989; Roelofs et al., 1992). As mechanisms responsible for these effects, electrostatic interaction between the negatively charged Q_A^- and $Pheo^-$ (van Mieghem et al., 1995) or changes of local protein conformation (van Mieghem et al., 1992) have been proposed. On the other hand, several observations indicate that strongly reducing conditions can cause double reduction of Q_A and that this state is probably stabilized by double protonation leading to the electrically neutral state Q_AH_2 (van Mieghem et al., 1992, 1994, 1995; Vass et al., 1992; Liu et al., 1993). Such a state with blocked forward electron transfer but electrostatic conditions similar to open RCs should be well suited for determination of the intrinsic rate constant of charge recombination of the primary pair.

The efficiency of creation and stability of the RP in various experiments with blocked electron transfer from $Pheo^-$ to Q_A has been usually assessed by two quantities discussed in the literature: RP yield and lifetime. As the RP is a transient state, its yield is not easily defined. The definition adopted in the following is the maximum transient concentration of the radical pair (RP_{max}) relative to the number of photons absorbed at low excitation energy. The RP lifetime τ is the apparent time constant in the exponential function $\exp(-t/\tau)$, which fits the RP decay deduced from the analysis of the experimental kinetics. These quantities were examined by several groups mainly for samples with singly reduced Q_A (Q_A^- state) (Nuijs et al., 1986; Schatz et al., 1987, 1988; Schlodder and Brettel, 1988; Hansson et al., 1988; Leibl et al., 1989; Liu et al., 1993; van Mieghem et al., 1995) but also for samples with doubly reduced Q_A (referred to in this paper as Q_AH_2 state) (Liu et al., 1993; van Mieghem et al., 1995). The results of these studies are ambiguous. Reported RP yields at room temperature for the Q_A^- state vary from 10% (Leibl et al., 1989) to 60% (Schlodder and Brettel, 1988) depending on the antenna size, species, and probably the procedure of preparation and the experimental method. At low temperature (20 K), a RP yield of 100% has been determined (van Mieghem et al., 1995). The published values of the RP lifetime in the Q_A^- state at room temperature vary from ~1 ns (Leibl et al., 1989) to 11 ns (Schlodder and Brettel, 1988) or even longer (Takahashi et al., 1987; Hansson et al., 1988; Liu et al., 1993). In samples with Q_A doubly reduced (in core complexes from *Synechococcus* containing ~40 chlorophyll molecules per RC), van Mieghem et al. (1995) reported at room temperature a RP lifetime of 13 ns and a yield of 100%. Liu et al. (1993) measured the RP decay of PS II core complexes from spinach in this state to be biphasic with lifetimes of 4 ns (40%) and 30 ns (60%). It is worth noting that RP lifetimes measured in isolated RCs are generally longer than in more intact preparations and extend to several tens of nanoseconds (Takahashi et al., 1987; Hansson et al., 1988; Booth et al., 1991).

In most kinetic studies of the primary RP in PS II, absorption change measurements or fluorescence decay measurements have been applied. Both techniques have some drawbacks. In the former a limited time resolution and/or contribution from excited states often do not allow correct measurements of the fastest decay components. With pump-probe techniques, lifetimes longer than a few nanoseconds are difficult to detect due to the limitations in the delay time. Fluorescence measurements might suffer from contributions from unconnected antenna chlorophylls or they might, in the case of a distribution or relaxation of radical pair states, over-represent the states lying energetically closer to the excited state. In addition, fluorescence measurements do not give any direct information on the RP yield. The latter can in principle be determined from molecular rate constants; however, even with global target analysis it is difficult to obtain unambiguous results (Roelofs et al., 1992).

Direct detection of RP formation and decay by time-resolved photovoltage measurements is an attractive alternative that can give complementary information. In the present work we applied a fast photovoltage technique (Wulf and Trissl, 1995; Trissl and Wulf, 1995) that allows selective measurements of yield and dynamics of the electrogenic states $P680^+Pheo^-$ and $P680^+Q_A^-$. The main aim was to investigate the effect of electrostatic interactions

within the RC protein on primary charge separation and recombination. From the photovoltage response after inhibition of charge stabilization, it is possible to determine both the relative yield of RP formation (from the amplitude) and the lifetime of the RP (from the decay time of the signal). These quantities are compared for the states Q_A^- and Q_AH_2. On the basis of a first-order reversible reaction scheme (Scheme 1, below), molecular rate constants and free energy differences between the state $P680^+Pheo^-$ and the equilibrated excited state $(Chl_NP680)^*$ for the three redox states of Q_A are calculated and discussed.

MATERIALS AND METHODS

Sample preparation

PS II membrane fragments were prepared from spinach according to the procedure described by Berthold et al. (1981) with slight modifications. To obtain single, destacked membrane fragments suitable for electrical orientation, a mild trypsin treatment was performed on the sample (Leibl et al., 1989; Pokorny, 1994). Concentrated PS II membranes (4 mg of chlorophyll/ml) were diluted in a buffer containing 10 mM 2-[*N*-morpholino]ethanesulfonic acid (MES) (pH 6.0), 10 mM NaCl, and 0.3 M sucrose to a final chlorophyll concentration of 100 μg/ml. Then trypsin (Sigma Chemical Co., St. Louis, MO) was added from a stock solution (5 mg/ml in 20 mM $CaCl_2$) to yield a concentration of 2 μg/ml. After 5 min of incubation in the dark at room temperature, the proteolysis was stopped by addition of a fivefold excess of trypsin inhibitor (Sigma) from a stock solution (10 mg/ml in 20 mM $CaCl_2$). The solution was then centrifuged (20,000 $\times$ *g*, 10 min, 4°C), and the pellet was washed several times in a low ionic strength buffer containing 2 mM MES, pH 6.0, 2 mM NaCl, and 0.3 M sucrose. The final chlorophyll concentration was ~4 mg/ml. The trypsin treatment was always performed less than 1 day before experiments, and the sample was kept on ice until use. Control measurements of fluorescence kinetics on membranes not trypsinized show no significant differences compared with trypsinized samples in any of the three redox states of Q_A. This indicated that the primary reactions were not modified by the trypsin treatment.

Q_A oxidation was achieved by addition of 10–100 μM potassium ferricyanide and ~10 min dark adaptation before the measurements. Single reduction of Q_A was obtained by addition of 40 mM sodium dithionite. Alternatively, we applied a saturating preflash or a weak background illumination after addition of 100 μM 3-(3,4-dichlorophenyl)-1,1-dimethylurea (DCMU). Double reduction of Q_A was performed by addition of 40 mM sodium dithionite followed by illumination with white light (~30 mW/cm^2 for 10 min). After the illumination the sample was kept in darkness for ~40 min to allow for reoxidation of photoaccumulated $Pheo^-$. All preparation steps were performed with degassed buffers under argon atmosphere. The control experiments for verification of the reduced states of Q_A will be discussed below.

Fluorescence measurements

Fluorescence kinetics were measured on samples (chlorophyll concentration ~2 mg/ml) placed in a flat glass cuvette with an optical path length of 1 mm. Excitation was by flashes from a frequency-doubled picosecond Nd-YAG laser (532 nm, 20 ps; Continuum, Santa Clara, CA). To minimize nonlinear effects (such as singlet-singlet annihilation) the energy density was reduced by neutral density filters to 10–100 μJ/cm^2. Fluorescence kinetics was detected with a microchannel photomultiplier (FWHM 150 ps; Hamamatsu, Hamamatsu City, Japan) and a 7-GHz digitizing oscilloscope (IN7000, Intertechnique, Les Ulis, France). The detection wavelength was selected by an interference filter centered at 680 nm. The apparatus response was determined by measuring the response to 20-ps flashes of green scattered light. The fluorescence traces were fitted by a sum of two or three exponential components $FL(t) = \Sigma_{i=1}^{n} a_i \exp(t/\tau_i)$, $n = 2$ or 3, convoluted with the apparatus response. The values of the parameters a_i

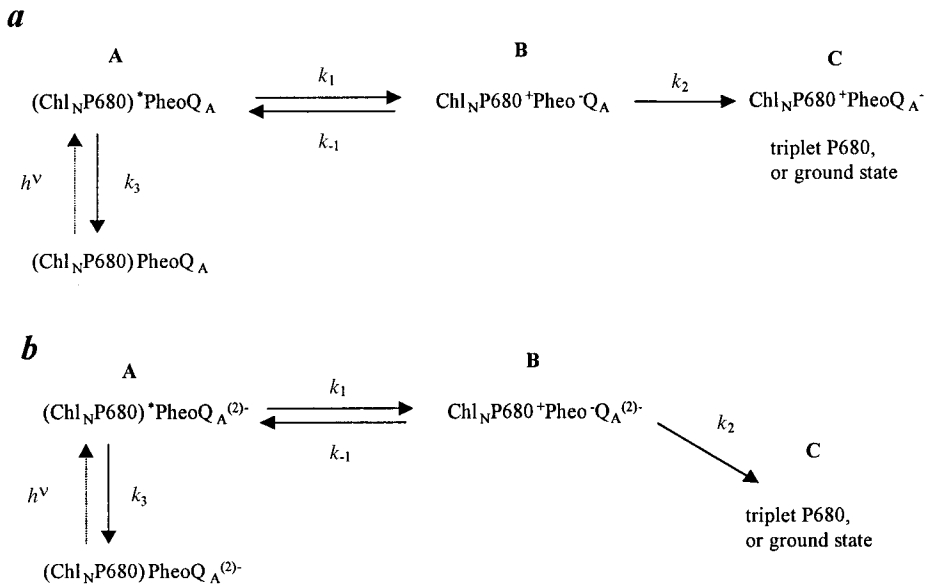

SCHEME 1 Reversible reaction schemes according to the exciton/radical pair equilibrium model (Schatz et al., 1988) for PS II with Q_A oxidized (*a*) and singly or doubly reduced (*b*). A, B, and C denote the respective states. $(Chl_NP680)^*$ designates the excited state equilibrated between *N* antenna chlorophylls and P680. Molecular rate constants are as follows: k_1, rate for primary charge separation; k_{-1}, rate for RP recombination with repopulation of the excited state; k_2 in *a*, overall rate for charge stabilization and for recombination to the ground or triplet P680 state; k_2 in *b*, rate for primary RP recombination reactions not repopulating the excited state; k_3, rate for decay of excited states (fluorescence emission and radiationless deactivation).

and τ_i were determined by a fit procedure minimizing the sum of the unweighted squared residuals.

Time-resolved photovoltage measurements

A detailed description of the photovoltage technique has been given elsewhere (Wulf and Trissl, 1995; Trissl and Wulf, 1995). Briefly, the transmembrane electron transfer during primary charge separation builds up a membrane potential, which can be detected as a photovoltage signal if the sample in the capacitative measuring cell is oriented. The sample (chlorophyll concentration ~4 mg/ml) was placed in a small coaxial cell between two platinum electrodes (Trissl and Wulf, 1995). The destacked PS II membranes were oriented in multilayers on the lower electrode by applying a short electric pulse (~200 ms, 800 V/cm). From the amplitude of the photovoltage upon a saturating flash (~300 mV) it can be estimated that this procedure leads to effective orientation of ~10 layers of membranes stacked on top of each other. In the case of experiments with samples in the states Q_A^- and Q_AH_2, chemical reduction was achieved after electrical orientation by adding a reducing buffer under an argon atmosphere. Excitation was as in the fluorescence experiments. For detection of the photovoltage kinetics, a 6-GHz preamplifier (Nucletude, Les Ulis, France) and the same digitizing oscilloscope as for fluorescence measurements were used. The apparatus response was determined experimentally by measuring the ultrafast charge separation in oriented purple membranes from *Halobacterium halobium* (Trissl and Wulf, 1995; see *inset* in Fig. 2 *A*). The primary and secondary radical pair kinetics was modeled by a reversible reaction scheme (Scheme 1) that, in the low-energy limit, results in a function $PV(t)$ containing two exponential components with two apparent time constants and a relative amplitude A_2^{app} (Eqs. A1–A3 in the Appendix). The relations between these apparent parameters and the five molecular parameters (four molecular rate constants and the relative electrogenicity e_2/e_1; see below) are given by Eqs. A4–A6. The kinetic traces were analyzed by a convolution of the apparatus response and $PV(t)$ (see Trissl and Wulf, 1995). The apparent parameters were determined by an iterative fit procedure as described before for analysis of the fluorescence kinetics.

RESULTS

Fluorescence and photovoltage kinetics were measured on destacked PS II membrane fragments pretreated to prepare them in three different initial redox states of Q_A: oxidized, singly reduced, and doubly reduced. Fluorescence decay kinetics in these redox states have been reported by several groups on comparable samples using a single photon-counting technique (van Mieghem et al., 1992; Vass et al., 1993). It has been demonstrated that the fluorescence decay kinetics are characteristic of the redox state of Q_A. On the basis of these published data, the fluorescence measurements in this work were primarily performed to serve as a tool and control of establishment of the desired redox states of the sample.

Fluorescence kinetics

Fig. 1 shows typical fluorescence kinetics detected for the samples with Q_A oxidized, Q_A singly reduced, and Q_A doubly reduced (see Materials and Methods). For comparison, the experimental traces are normalized to equal initial amplitudes. The parameters resulting from a fit by a sum of two or three exponential functions are given in Table 1. Taking into account the limited time resolution of the fluorescence measurements in this work, our results agree fairly well with the more precise data from single photon-counting experiments (Table 1) (van Mieghem et al., 1992; Vass et al., 1993). In agreement with the observations reported in the literature, kinetics in the states Q_A and Q_AH_2 are dominated by fast phases of ~100–200 ps, whereas in the state Q_A^- a slower phase of ~1.5 ns is dominant. In the state Q_AH_2 there is a very slow phase of 6 ns, which is not present in the two other redox states of Q_A. For preparation of the doubly reduced state, we optimized the conditions (time and intensity of illumination, dark re-adaptation time, and concentration of sodium dithionite) so as to obtain fluorescence kinetics with a maximum contribution of the 6-ns component (see Discussion). The double reduction of Q_A was almost completely reversible after addition of 10 mM ferricyanide (data not shown).

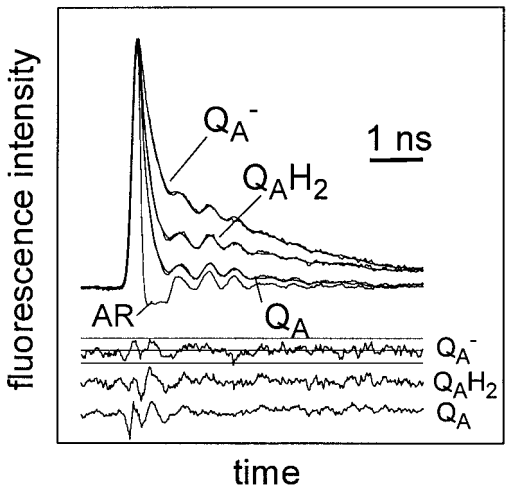

FIGURE 1 Fluorescence kinetics (λ = 680 nm) of PS II membrane fragments with Q_A in three different initial redox states as indicated. Best fits obtained by convolution of a multiexponential decay and the apparatus response function are superimposed on the experimental traces. The three lower traces are plots of deviations between calculated and experimental traces (residual plots) with upper and lower straight lines indicating ±2% deviation. AR, apparatus response to 20-ps flashes of green scattered light (FWHM, 150 ps).

Photovoltage kinetics

The same preparation and the same protocol to establish the initial redox states of Q_A as the one described above were used for photovoltage experiments. Fig. 2 *A* presents the photovoltage kinetics obtained upon excitation with a picosecond flash of the same oriented PS II membranes prepared successively with Q_A oxidized (Q_A) and either Q_A singly reduced (Q_A^-) or Q_A doubly reduced (Q_AH_2). Clear differences between the three traces are seen both in amplitudes and in kinetics. For better comparison of the kinetics in the

TABLE 1 Fluorescence decay components and relative fluorescence yields of PS II membranes in three different initial redox states of Q_A

Initial redox state	Reference	Fluorescence decay components				Relative yield, Φ (arbitrary units)
		τ_1 (a_1) (ns (%))	τ_2 (a_2) (ns (%))	τ_3 (a_3) (ns (%))	τ_4 (a_4) (ns (%))	
Q_A	This work	**0.12 (60)**	**0.37 (40)**			**0.22**
	van Mieghem et al., 1992	0.14 (73)	0.33 (27)	3.2 (0.04)		0.19
	Vass et al., 1993	0.08 (26)	0.20 (58)	0.39 (15)	2.2 (0.07)	0.20
Q_A^-	This work	**0.16 (40)**	**1.5 (60)**			**0.96**
	van Mieghem et al., 1992	0.60 (25)	1.4 (68)	3.3 (7)		1.33
	Vass et al., 1993	0.26 (23)	0.87 (31)	1.75 (41)	3.9 (4.9)	1.27
Q_AH_2	This work	**0.15 (61)**	**0.60 (30)**	**6.0 (9)**		**0.81**
	van Mieghem et al., 1992	0.22 (69)	0.60 (18)	2.0 (8)	7.1 (5)	0.77
	Vass et al., 1993	0.16 (67)	0.58 (24)	2.9 (6.8)	9.6 (1.8)	0.62

Relative yields are calculated as $\Phi = \Sigma_{i=1}^{n} a_i\tau_i$.

states Q_A^- and Q_AH_2, these traces were normalized in Fig. 2 *B*. Normalization was done by multiplying the photovoltage signal in the state Q_A^- (Fig. 2 *A*) by a constant so as to obtain the same maximal amplitudes for both traces.

Owing to the limited sensitivity of the photovoltage setup and the necessity of correlation of the results of both techniques, relatively high excitation energies ranging from 10 to 70 $\mu J/cm^2$ were applied for both fluorescence and photovoltage. In some experiments an even higher excitation energy, up to 100 $\mu J/cm^2$, was applied to record photovoltage signals in the state Q_A^- because of the low signal-to-noise ratio in this state. No significant differences were observed for excitation within this energy range. As shown in Fig. 3, the photovoltage generated by samples in the state Q_AH_2 for these energies is still in the linear range of the saturation curve. This justifies the application of the simplified model, which neglects nonlinear effects (Scheme 1) for a quantitative analysis of photovoltage results.

In the case of initially oxidized Q_A, not only the transient primary radical pair ($P680^+Pheo^-$) is monitored, but also subsequent formation of the secondary radical pair ($P680^+PheoQ_A^-$) leads to a further increase of the membrane potential and appears as a second positive electrogenic step in the photovoltage. According to a two-step sequential forward reaction the photovoltage in samples with oxidized Q_A increases biphasically, reaches its maximum value at ~2–3 ns after the flash, and is stable on the time scale of the measurement (5–10 ns). Both radical pair states involved are weighted with electrogenicity factors, which reflect the (dielectrically weighted) transmembrane distances between the separated charges (Eqs. A3 and A4). As it has been shown previously, the electrogenicity factor of the secondary radical pair is about twice as large as the one of the primary radical pair, indicating a transmembrane position of Pheo about midway between P680 and Q_A (Leibl et al., 1989; Pokorny, 1994).

Single reduction of Q_A before the flash by addition of dithionite (Fig. 2 *A*, trace Q_A^-) causes a drastic decrease in the photovoltage amplitude and a completely different shape of the kinetics. As expected, the second rising phase, due to Q_A reduction, is lost and replaced by a back-reaction. In addition, the amplitude of the photovoltage signal is diminished compared with that for the samples with oxidized Q_A by much more than the expected factor of two, indicating a significant reduction of the yield of RP formation.

Double reduction of Q_A by illumination and subsequent dark incubation of dithionite-treated samples (Fig. 2 *A*, trace Q_AH_2) leads to a strong increase of the amplitude of the photovoltage signal relative to the trace Q_A^-. The increase in the amplitude is accompanied by a slower decay of the photovoltage. It is necessary to stress that this evolution does not result from reoxidation of Q_A^- in part of the centers, which would lead to a mixture of Q_A and Q_A^- states and consequently could give rise to a similar effect of apparent slower decay and increased amplitude. To exclude this possibility two tests were performed that, if some reoxidation of Q_A^- had occurred, would regenerate the state Q_A^-. The tests consisted in either application of continuous background light or in re-addition of freshly prepared dithionite to the sample. Neither of these control experiments showed a significant change (acceleration of the decay or decrease of the amplitude) of the photovoltage response, thus demonstrating that reoxidation of Q_A was not the origin of the observed changes. It can therefore be concluded that the described photovoltage response is characteristic of RCs with doubly reduced Q_A. Qualitatively, it indicates that in samples with doubly reduced Q_A the yield of RP formation and the lifetime of the RP are increased relative to those for the samples with singly reduced Q_A.

Kinetic analysis of the photovoltage data revealed that the kinetics in all three redox states of Q_A could be well fitted with two exponential components (Eq. A3). The results of this analysis are collected in Table 2. In the state Q_A the relative amplitude A_2^{app} equals 3.4 (corresponding to an electrogenicity of the state $p^+Q_A^-$ of ~1.85 relative to the electrogenicity of the state p^+ $Pheo^-$ (see below); Eq. A4),

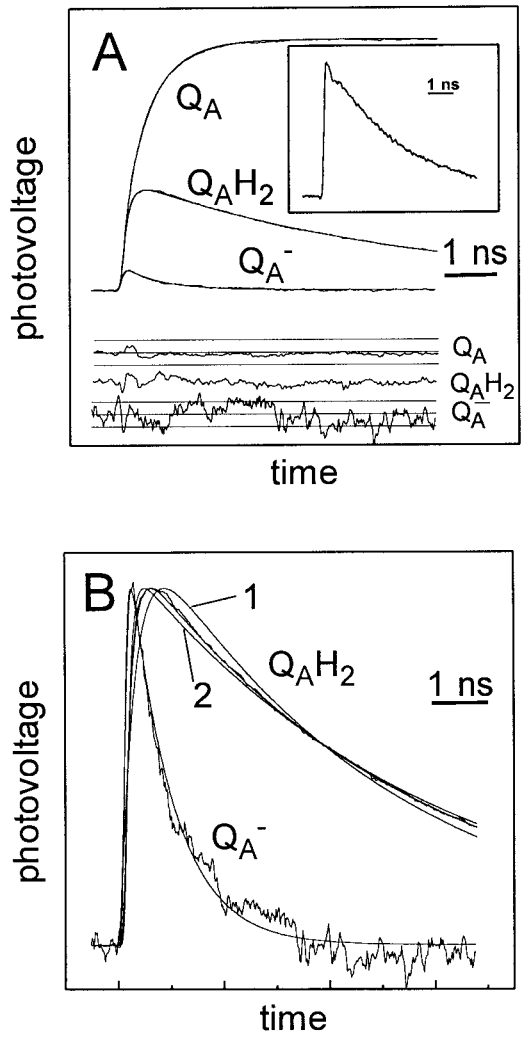

FIGURE 2 (*A*) Photovoltage kinetics of PS II membrane fragments with Q_A in three different initial redox states as indicated. An exponential decay due to the apparatus response (*inset*) has been deconvoluted for clearer presentation. Best fits are superimposed on the experimental traces and residual plots are shown below with upper and lower straight lines indicating ±2% deviation for the states Q_A and Q_AH_2 and ±5% deviation for the state Q_A^-. (*Inset*) Photovoltage kinetics of purple membranes used to determine the exponential decay due to the apparatus response used for deconvolution. (*B*) Photovoltage traces for the states Q_A^- and Q_AH_2 with best fits superimposed and normalized to the same maximal amplitude. Additionally, for the state Q_AH_2 two model curves (*1* and *2*) are presented obtained by fixing $k_1 = 2\ ns^{-1}$ (*trace 1*) or $k_1 = 10\ ns^{-1}$ (*trace 2*) and optimizing k_{-1} and k_2 to obtain the best fit. k_3 was fixed to $1\ ns^{-1}$ (set 1, Table 3). As can be seen, values of k_1 different from those in Table 3 do not allow a fit to the experimental traces. In the states Q_AH_2 and Q_A, similar deviations can be observed (not shown) when fixing the values of other molecular rate constants outside the ranges given in Table 3. In the state Q_A^-, fixing one molecular rate constant outside the range of values in Table 3 may be compensated by the other rate constants so that the experimental trace can be well fit. However, in these cases other constraints (e.g., relative peak amplitude of the photovoltage signal; see Appendix 2) would be violated.

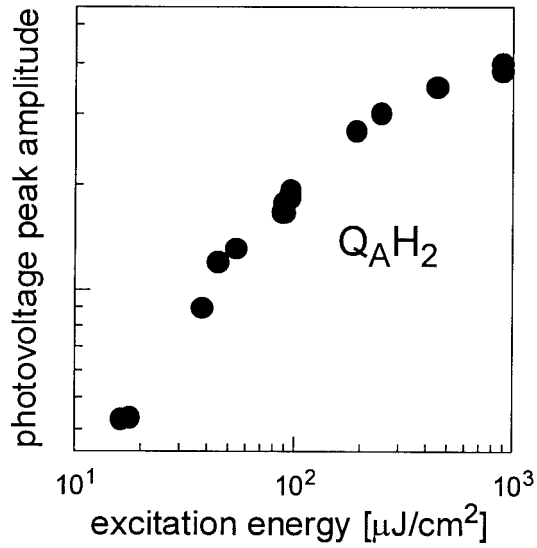

FIGURE 3 Double logarithmic plot of the dependence of the peak amplitude of the photovoltage response in the state Q_AH_2 on the excitation energy. The measurements used for kinetic analysis were performed at an excitation energy of less than 100 $\mu J/cm^2$.

and the time constants of the two phases were $\tau_1 = 220$ ps and $\tau_2 = 620$ ps. These time constants are in good agreement with values of 170 ps and 520 ps measured for PS II membranes from peas (Leibl et al., 1989). The kinetics in the state Q_AH_2 is characterized by a similar time constant for formation of the primary RP ($\tau_1 = 180$ ps) and a time constant of $\tau_2 = 5.5$ ns for its decay. The data are well fitted by a value of $A_2^{app} = -1$ (corresponding to $e_2/e_1 = 0$; Eq. A4), which is expected for a monophasic radical pair recombination process. The peak amplitude of the photovoltage signal observed in different experiments ranged from 30% to 46% of the one observed on the same preparation with oxidized Q_A. These values may be underestimated due to a slight loss of amplitude, which could be caused by the procedure of dithionite addition disturbing somewhat the orientation of the sample. However, it is clear that the amplitude in the state Q_AH_2 was significantly (about five

TABLE 2 Apparent time constants and relative amplitudes, A_2^{app}, of the photovoltage response from PSII membranes in three different initial redox states of Q_A

Initial redox state	Kinetics components			Relative peak amplitude (%)
	τ_1 (ns)	τ_2 (ns)	A_2^{app}	
Q_A	0.22 ± 0.03	0.62 ± 0.03	3.4 ± 0.1	100
Q_A^-	0.05 ± 0.02	0.80 ± 0.30	−1	8 ± 2
Q_AH_2	0.18 ± 0.02	5.5 ± 0.5	−1	38 ± 8

$A_2^{app} = 3.4$ corresponds to a relative electrogenicity $e_2/e_1 = 1.85$ (Eq. A4). Values were obtained by a best fit according to Eq. A3. The relative peak amplitudes of the photovoltage responses (after deconvolution of the apparatus response function) are given in the right column.

times) higher when compared with that obtained for the state Q_A^-. It is worth noting that the transition from the single to the doubly reduced state did not require a change of the redox buffer solution covering the stacked membrane layer in the measuring cell (such a buffer change is necessary for the transition from the oxidized to the single reduced state; see Materials and Methods) but was realized only by the application of continuous light. Therefore, the observed increase of the amplitude by a factor of five when going from the state Q_A^- to Q_AH_2 is clearly due to an increased yield of RP formation. The kinetics in the state Q_A^- is characterized by a rising phase of ~50 ps and a decay phase of 800 ps, both time constants being significantly faster than in the case of doubly reduced Q_A. As in the case of Q_AH_2, a relative amplitude of $A_2^{app} = -1$ fit well in the analysis. It is interesting to note that on the basis of a simple phenomenological description by two consecutive reactions the decrease in the maximum RP concentration in the state Q_A^- could be easily explained by assigning the 800-ps component to the formation of the RP and the 50-ps component to its decay. A more detailed analysis in terms of molecular rate constants will be given below.

DISCUSSION

Preparation of the redox states of Q_A

In general, the methods of preparing samples with Q_A oxidized and singly reduced seem well established. The oxidized state is the one that is easiest to obtain in pure form. To assure that all RCs were in the state Q_A, a small amount (up to 100 μM) of potassium ferricyanide was added to the sample in addition to dark adaptation. This artificial electron acceptor reoxidizes residual Q_A^- between flashes during data acquisition.

Preparation of samples with all Q_A singly reduced is more difficult. It was suggested, for example, that addition of sodium dithionite could cause some double reduction of Q_A already in the dark, although more purified preparations such as core complexes seem to be more susceptible to this than the intact membrane preparations used in this work (van Mieghem, 1994). Single reduction of Q_A could in principle be performed also by a preillumination of the sample in the presence of DCMU, an inhibitor of reoxidation of Q_A^- by electron transfer to Q_B. However, it was found that chemical reduction gives the most reliable results. The other methods (DCMU plus saturating preflash or continuous background light) might leave Q_A in the oxidized state in a small fraction of RCs. On the other hand, due to the instability of sodium dithionite there remains also some uncertainty about the establishment of a stable Q_A^- state by chemical reduction. Fortunately, the very properties of the photovoltage response offer sufficient arguments against a significant contribution from the states Q_A and Q_AH_2. The characteristic kinetics and especially the very small amplitude are inconsistent with a significant contribution of the other states, which are characterized by quite different kinetics and much larger amplitudes. On the other hand, because the signal from the state Q_A^- is small, even minor contamination by the larger signal from the other redox states would distort it significantly. However, simulations show that such a contamination would clearly manifest itself by the presence of a slow component in the photovoltage decay (5.5 ns or a constant). This is not observed. Furthermore, the fluorescence kinetics for the states Q_A and Q_A^- (Fig. 1; Table 1) agreeing well with those in the literature (Hodges and Moya, 1986; Schatz et al., 1988; Leibl et al., 1989; van Mieghem et al., 1992; Vass et al., 1993) also confirm the validity of the methods of preparation of the different redox states.

To verify the preparation of the state Q_AH_2, we compared our fluorescence kinetics to published data (Table 1) for the same kind of preparation, i.e., PS II membrane fragments from spinach (van Mieghem et al., 1992; Vass et al., 1993). These data had been obtained by the technique of single photon counting and analyzed with four exponential functions. The published characteristics of the fluorescence decay kinetics in the state Q_AH_2 are very similar to those presented in this paper with a dominant fast phase (150–220 ps), a middle component of smaller contribution (~600 ps), and a very slow phase (7–10 ns). Irrespective of the number of kinetic phases and their exact lifetimes, it appears clearly that the relative fluorescence yields, Φ, for the three redox states of Q_A (Table 1) are in good agreement with literature data. Compared with the oxidized state, the values of Φ increase by about a factor of 6 and 3–4 for the singly and doubly reduced state, respectively. In the work of van Mieghem et al. (1992), fluorescence experiments were performed on samples for which the redox state of Q_A was monitored by electron paramagnetic resonance (EPR). PS II membranes with Q_A singly reduced showed a large Q_A^- EPR signal, which was absent both in samples with Q_A oxidized and in samples doubly reduced. Based on the correlation of the Q_A redox state monitored by EPR and the fluorescence kinetics characterized by van Mieghem et al. (1992) we used in our work the presence of a long (6–10 ns) fluorescence component with significant amplitude, together with the large amplitude of the fast phase (60–70%) and the value of $\Phi(Q_AH_2)/\Phi(Q_A) = 3–4$ as indicators for the state Q_AH_2.

Molecular rate constants

In principle, fluorescence and photovoltage data give complementary kinetic information, and the experimental parameters (lifetimes and amplitudes) from both techniques could be used to determine molecular rate constants. In the framework of Scheme 1 the kinetics in all redox states of Q_A should be characterized by two exponential phases, and the values for time constants for photovoltage and fluores-

cence kinetics should be identical (see Appendix 1). However, some time constants measured by fluorescence, both in this work and in work by other authors, are significantly different from time constants measured by photovoltage (compare Tables 1 and 2). This is the most evident in the state Q_AH_2, where more than two phases are necessary to describe the fluorescence decay. But also in the other states some differences, especially concerning the time constant of the fast phases, are observed.

The reason for these discrepancies is probably that Scheme 1 is too simple to give a correct description of the fluorescence kinetics because it does not take into account additional reaction steps that are expected to give additional kinetic phases of fluorescence decay. Several studies of PS II preparations with high temporal and amplitude resolution reported fluorescence decay kinetics with more than two phases (Roelofs and Holzwarth, 1990; van Mieghem et al., 1992; Roelofs et al., 1992; Vass et al., 1993). These results were interpreted either in terms of heterogeneity of photosystems (contribution of PS I and/or different behavior of PS IIα and PS IIβ; Roelofs et al., 1992) or in terms of a relaxation of the primary radical pair (Vass et al., 1993, Yruela et al., 1996). The samples used in this work contain no detectable amounts of PS I and, judged from the values for molecular rate constants determined from the photovoltage kinetics, resemble PS IIβ (see below). In other words, the photovoltage response probably originates from a homogeneous sample. It is not completely sure that this applies also to the fluorescence response, which could possibly contain a contribution from still stacked PS II membranes behaving like PS IIα.

Concerning a possible relaxation of the primary pair, the doubly reduced state should be the one in which it is the most easily detectable due to the long lifetime of the RP in this state. In fact, fluorescence transients in this state showed a third phase of ~600 ps, which could correspond to an energetic relaxation of the primary RP. The photovoltage kinetics, however, which monitors directly the time dependence of the radical pair concentration, was well described by a single decay time. This could mean that within the precision of the photovoltage measurements, a possible radical pair relaxation is not connected with sufficient change in electrogenicity (due to charge movement perpendicular to the membrane plane) to be observed.

Another additional reaction step that is neglected in Scheme 1 is exciton equilibration within the PS II antenna complexes. Such processes had been detected as fast fluorescence phases (15–20 ps) of significant relative amplitude (0.35), both for open and closed RCs (McCauley et al., 1989; Roelofs et al., 1992). The fluorescence data in the present work were not of sufficient precision to resolve such phases. As a consequence the lifetimes and amplitudes of the faster fluorescence phases observed in this work may be distorted.

The additional reaction steps discussed above, like exciton equilibration and primary radical pair relaxation, are expected to affect fluorescence much more than photovoltage kinetics, for which Scheme 1 seems sufficient. Certainly a global analysis of kinetic data from both techniques would be the best approach. However, the use of a more complicated reaction scheme makes it impossible to determine all involved molecular rate constants. For these reasons the analysis presented in the following will be mainly based on the photovoltage data and the simple scheme (Scheme 1).

One advantage of the photovoltage is that the amplitudes give information about relative concentrations of the RP, which can be compared for different redox states. This allows us to derive an important conclusion about the rate constant of primary charge separation independently of the other molecular rate constants. As can be seen from Eq. A7 the maximum concentration of the RP depends only on k_1 and the directly measured quantities τ_1 and τ_2. Taking into account the relative amplitudes of the photovoltage traces in the states Q_AH_2 and Q_A^- as well as the apparent rates (Table 2), the ratio $k_1(Q_AH_2)/k_1(Q_A^-) \approx 1.25$ can be deduced. This is an important result, which does not imply any assumptions. It demonstrates that the molecular rate constants of primary charge separation in the singly and doubly reduced state are comparable.

To determine the sets of molecular rate constants for the three redox states of Q_A we used two mathematical approaches (Appendix 2), both leading essentially to the same results (Table 3; compare results in sets 1 and 2 with those in set 3). As even with the simplified scheme, an attempt to determine precise values of the molecular rate constants would necessitate too many assumptions we rather restricted the analysis to the determination of the ranges of their possible values.

Most of the molecular rate constants are sufficiently well defined to allow drawing conclusions about the effect of the redox state of Q_A. Inspection of the values determined for k_1 and k_{-1} (in all three sets in Table 3) reveals the interesting result that the rate of RP recombination, k_{-1}, is strongly dependent on the redox state of Q_A, being similar for Q_A and Q_AH_2 but more than one order of magnitude higher for Q_A^-. On the other hand, the molecular rate constant for primary charge separation, k_1, is rather independent of the redox state of Q_A. This result contrasts with the result of kinetic analysis of time-resolved fluorescence (and transient absorption changes) from the literature. On a PS II preparation from *Synechococcus sp.* with 80 Chl/RC, the single reduction of Q_A was found to affect k_1 much more than k_{-1} (Schatz et al., 1988), and a similar result has been obtained in other works using fluorescence techniques (Roelofs et al., 1992; Vass et al., 1993). A possible reason for this difference may be the heterogeneity of PS II. In a very detailed study of picosecond chlorophyll fluorescence from pea chloroplasts, global target analysis allowed detection of a distinctly different behavior of β-centers compared with

TABLE 3 Sets of parameters calculated from photovoltage data for the three redox states of Q_A on the basis of Scheme 1

	Q_A	Q_A^-	Q_AH_2
1. $k_3 = 1.0\ ns^{-1}$			
k_1 (ns^{-1})	**3.0** (2.6–3.4)	**3.2** (2.0–4.4)	**3.9** (3.4–4.4)
k_{-1} (ns^{-1})	**0.52** (0.42–0.62)	**20** (10–30)	**0.8** (0.45–1.15)
k_2 (ns^{-1})	**1.75** (1.7–1.8)	**<2.3**	**<0.2**
RP_{max} (%)		**10** (7–13)	**62** (58–66)
a_2^{fl}	**0.22** (0.21–0.23)	**0.87** (0.84–0.90)	**0.10** (0.05–0.15)
Φ^{fl}	**0.30** (0.27–0.33)	**0.88** (0.80–0.96)	**0.69** (0.45–0.93)
Y_{CS} (%)	**70** (68–72)		
$\Delta G°$ (meV)	**−44** (−49–−41)	**+46** (+41–+57)	**−40** (−60–−38)
2. $k_3 = 0.4\ ns^{-1}$			
k_1 (ns^{-1})	**3.8** (3.4–4.2)	**4.0** (2.5–5.5)	**4.4** (3.8–5.0)
k_{-1} (ns^{-1})	**0.3** (0.2–0.4)	**16** (7–25)	**1.3** (0.6–2.0)
k_2 (ns^{-1})	**1.75** (1.70–1.80)	**4.9** (3.6–6.2)	**<0.2**
RP_{max} (%)		**13** (11–15)	**70** (65–75)
a_2^{fl}	**0.14** (0.13–0.15)	**0.86** (0.82–0.90)	**0.15** (0.07–0.22)
Φ^{fl}	**0.28** (0.25–0.31)	**0.88** (0.80–0.96)	**0.98** (0.50–1.46)
Y_{CS} (%)	**89** (87–91)		
$\Delta G°$ (meV)	**−65** (−68–−63)	**+38** (+30–+46)	**−45** (−60–−30)
3. Weak constraints			
k_1 (ns^{-1})	**2.8** (2.2–3.4)	**3.3** (2.8–3.8)	**4.2** (3.6–4.8)
k_{-1} (ns^{-1})	**0.7** (0.4–1.0)	**15** (12–17)	**0.6** (0.5–0.7)
k_2 (ns^{-1})	**1.75** (1.50–2.00)	**<5**	**<0.2**
k_3 (ns^{-1})	**1.0** (0.4–1.6)	**1.0** (0.4–1.6)	**1.0** (0.4–1.6)
RP_{max} (%)		**14** (12–16)	**67** (57–77)
$\Delta G°$ (meV)	**−36** (−52–−20)	**+37** (+29–+45)	**−67** (−77–−57)

k_i, molecular rate constants; RP_{max}, maximum transient concentration of the primary radical pair; a_2^{fl}, fluorescence amplitude of slower decay component; Φ^{fl}, fluorescence yield; Y_{CS}, the yield of charge stabilization; $\Delta G°$, standard free energy difference between the states $P680^+Pheo^-$ and $(Chl_NP680)*$. See text for further details.

that of α-centers (Roelofs et al., 1992). Upon single reduction of Q_A in PS IIβ, k_1 decreased by a factor of 3, but k_{-1} increased by a factor of 5. A previous study based on photovoltage (and fluorescence) kinetics on destacked PS II membranes revealed a similar change of the values of k_1 and k_{-1} upon single reduction of Q_A with a reduction of k_1 by a factor of 3 and an increase of k_{-1} by about a factor of 8 (Leibl et al., 1989). This resembles a behavior proposed for PS IIβ although the membranes had been prepared from PS IIα containing grana fragments. In thylakoids, PS IIα is located in the stacked grana region of the thylakoids, whereas PS IIβ is located in the unstacked stroma regions, and evidence for a reversible conversion of PS IIα to PS IIβ has been reported, probably connected with migration of PS II from grana to stroma region (Sundby et al., 1986; Guenther and Melis, 1990). It is possible that such a conversion takes place upon destacking of the grana membranes. It should be noted that in the photovoltage study mentioned above (Leibl et al., 1989), double reduction of Q_A had neither been studied nor considered. It is therefore likely that part of the difference between the results of this work and those reported by Leibl et al. (1989) can be attributed to the contribution of some doubly reduced Q_A in the presumed Q_A^- state in the earlier study.

The rate k_2 is not very well defined in the state Q_A^- (Table 3). This is mainly due to the fact that k_{-1} in this state is very high and that both reactions (described by k_2 and k_{-1}) compete in the depopulation of the radical pair state. However, all three sets show that in the state Q_AH_2, k_2 is smaller than 0.2 ns^{-1}. This may serve as an estimation of the upper limit for the recombination rate in open RCs (state Q_A) of the primary radical pair directly or via the triplet state of P680 to the ground state. The relatively small value of 0.2 ns^{-1}, compared with k_2 (Q_A) = 1.75 ns^{-1}, is in line with an efficient charge stabilization in open RCs (Kramer and Mathis, 1980; Thielen and van Gorkom, 1981; Schatz et al., 1988).

The rate constant for nonphotochemical decay, k_3 (Table 3, set 3) also shows a large range of values, which are compatible with the measured quantities and the constraints. This rate, like k_2 in closed RCs, describes a wasteful loss reaction, and variation of this rate has only relatively weak effects on the other molecular rate constants. The most significant effect of an increase of k_3 is a drop of the quantum yield of charge stabilization in open RCs. The range for k_3 determined in set 3 covers the two values used for calculation of sets 1 and 2.

To demonstrate the influence of the determined molecular rate constants on other observable quantities, some additional values are given in Table 3. The calculated maximum transient concentrations of the primary radical pair, RP_{max} (Eq. A7), in the states Q_A^- and Q_AH_2 are expressed in percentages of the initially absorbed photons per RC and may be compared to the RP yields from the literature (see

Introduction). For sets 1 and 2 also theoretical values for relative fluorescence amplitudes, a_2^{fl}, and fluorescence yields, Φ^{fl}, are calculated according to Eq. A12. These fluorescence quantities might be compared with the constraints related to fluorescence data that were used to calculate set 3 (see Appendix 2) showing that the constraints are justified. Only $a_2^{fl}(Q_A) = 0.14$ in set 2 is significantly lower than the corresponding constraint (0.25). However, as calculations show, a decrease of the lower limit for $a_2(Q_A)$ to 0 affects significantly only the ranges of $k_{-1}(Q_A)$ in set 3 (0–1.6 ns^{-1}) and has no influence on the main conclusions. Finally, also the yields of charge stabilization in open RCs, Y_{CS}, calculated in sets 1 and 2 (Eq. A8) are in accordance with the corresponding constraint used for the calculation of set 3 ($Y_{CS} > 0.5$) and with literature data (Kramer and Mathis, 1980; Thielen and van Gorkom, 1981; Schatz et al., 1988).

The standard free energy of the primary charge separation

Knowledge of the values of the molecular rate constants for the forward and back reactions allows us to obtain information on the energetics of the charge separation reaction. The values of k_1 and k_{-1} define the free energy difference, $\Delta G°$, between the states $P680^+Pheo^-$ and $(Chl_NP680)^*$ in the intact photosystem:

$$\Delta G° = -k_B T \ln(k_1/k_{-1}), \quad (1)$$

where k_B is the Boltzmann constant and T is the absolute temperature. $\Delta G°$ is negative and of similar magnitude for the states Q_A and Q_AH_2, whereas for the state Q_A^- it is positive (Table 3), indicating a significant shift of the energetic equilibrium toward the (equilibrated) excited state. The latter result is consistent with the idea that a negative charge on Q_A leads to a destabilization of the state $P680^+Pheo^-$ due to repulsive electrostatic interaction. On the other hand, a similar driving force observed for charge separation in the oxidized and doubly reduced state indicates that the electrostatic repulsion has disappeared. This result confirms that upon double reduction the charges on Q_A are neutralized by double protonation (Vass et al., 1992; van Mieghem et al., 1992, 1994, 1995; Liu et al., 1993). It therefore appears that the state Q_A^- can be used to provide an internal modulation of the standard free energy of primary charge separation when compared with the oxidized or fully reduced state.

In the framework of the exciton/radical pair equilibrium model, the molecular rate of charge separation from the equilibrated excited state, k_1, is linearly related to the intrinsic molecular rate, k_1^{int}, which describes electron transfer within the RC from the excited primary donor, P680*, to the primary acceptor:

$$k_1^{int} = k_1 N^{eff}, \quad (2)$$

where N^{eff} is an entropy factor representing the effective number of chlorophylls over which the excitation is equilibrated. If all pigments are isoenergetic, N^{eff} equals the actual antenna size (in our case $N \approx 250$). By taking into account a slight difference in the wavelength of the maximum absorption between the primary donor P680 (680 nm) and the antenna chlorophylls (673 nm) and assuming a Boltzmann distribution of the excited states, N^{eff} is reduced to ~125 (see, e.g., Schatz et al., 1988). With the values for k_1 given in Table 3, k_1^{int} can be estimated at $(2–3\ ps)^{-1}$, in accordance with values reported for isolated RCs (Wasielewski et al., 1989; Roelofs et al., 1991; Chang et al., 1994; Schelvis et al., 1994; Müller et al., 1996; Greenfield et al., 1997). The standard free energy difference between the primary radical pair and P680*, $\Delta G°,^{int}$, is given by

$$\Delta G°,^{int} = -k_B T \ln(k_1^{int}/k_{-1}) = \Delta G° - k_B T \ln N^{eff}, \quad (3)$$

where for $N^{eff} = 125$ and at room temperature the last entropy term adds ~−120 meV to the free energy gap. The diagram in Fig. 4 presents, for the three redox states of Q_A, the calculated free energy differences for charge separation from the excited states $(Chl_NP680)^*$ and P680*. Fig. 5 is a logarithmic plot of the intrinsic molecular rate constants for the three redox states of Q_A (k_1^{int} and k_{-1}, Table 3) against the corresponding values of $-\Delta G°,^{int}$.

It should be emphasized that the values of $\Delta G°$ and $\Delta G°,^{int}$, as well as for all molecular rate constants, are calculated based on the simple exciton/radical pair equilibrium model (Scheme 1). This model accounts neither for a possible intermediate in electron transfer between P680 and Pheo nor for energetic relaxation of the primary radical pair. These phenomena exist in bacterial RCs (Woodbury and Parson, 1984; Peloquin et al., 1994; Holzapfel et al., 1989, 1990; Holzwarth and Müller, 1996), and the strong struc-

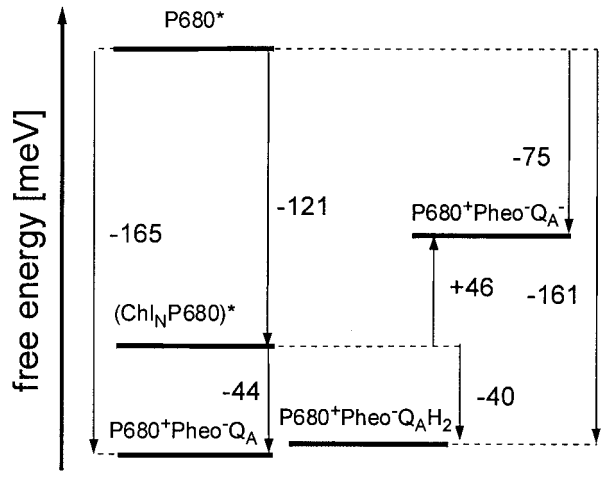

FIGURE 4 Calculated free energy differences for charge separation from the excited states $(Chl_NP680)^*$ and P680* in the states Q_A, Q_A^-, and Q_AH_2.

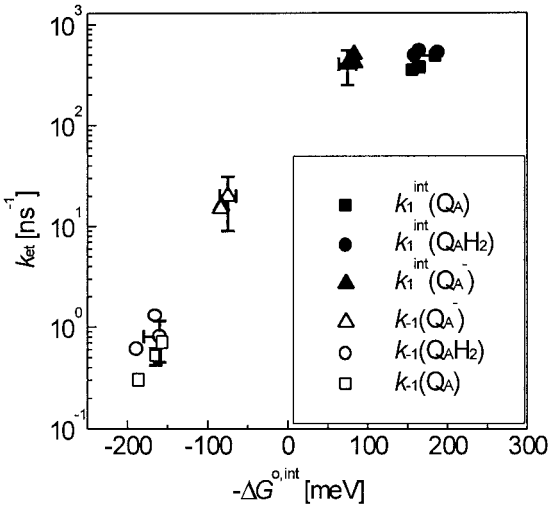

FIGURE 5 Dependence of the intrinsic molecular rate constants for charge separation (k_1^{int}) and charge recombination (k_{-1}) on the driving force $-\Delta G^{o,int}$ for the three redox states of Q_A (Q_A, Q_A^-, and Q_AH_2). Experimental points and representative error bars are from Table 3. The values of k_1^{int} and $\Delta G^{o,int}$ were calculated from Eqs. 2 and 3. Based on the simple exciton/radical pair equilibrium model it is assumed that the values of $\Delta G^{o,int}$ for back reactions equal $-\Delta G^{o,int}$ for forward reactions.

tural and functional similarity of PS II and purple bacterial RCs suggests that they may also exist in PS II, although this has not been established. Controversial interpretations about the existence of relaxation of the RP were given in papers describing primary reactions in PS II membranes (Roelofs and Holzwarth, 1990; Vass et al., 1993, Yruela et al., 1996) and in isolated RCs (Booth et al., 1991; Schelvis et al., 1994; Müller et al., 1996). During relaxation the free energy level of the primary radical pair decreases with time, most probably due to the dielectric response of the protein, and $-\Delta G^{o,int}$ increases. In this case the $-\Delta G^{o,int}$ for the forward and backward electron transfer would be different. However, if there is no intermediate, and relaxation for times shorter than several nanoseconds may be neglected, one could assume the reorganization energy λ and $|\Delta G^{o,int}|$ to be the same for the forward and backward reaction and fit the points in Fig. 5 with a Marcus parabola (Marcus, 1956; Marcus and Sutin, 1985). Such a fit would give a value for the reorganization energy λ of ~120 meV. In the framework of this analysis the weak dependence of the charge separation rate k_1^{int} on the redox state of Q_A (Fig. 5) is consistent with the activationless character of this reaction occurring with a rate near its optimum value ($\lambda = -\Delta G^{o,int}$). This is typical of primary charge separation reactions in photosynthetic RCs (Krishtalik, 1989).

CONCLUSIONS

The results of this work show that in intact PS II the yield of charge separation is strongly diminished when the primary quinone acceptor is singly reduced. This behavior might have a physiological role. Under high light conditions it minimizes formation of $P680^+$ and $^3P680$ (triplet form of P680) by fast charge recombination to the excited state. Fast recombination to the ground state is probably not a possible alternative for reactions within the RC, as the latter has to be optimized for high quantum yield of charge separation and stabilization under normal conditions. However, highly efficient, ΔpH-dependent quenching processes based on fast nonradiative dissipation of excitation energy exist in the antenna (Mullineaux et al., 1993). The prevention of $P680^+$ and $^3P680$ formation is essential in PS II because of the high oxidizing power of $P680^+$ and the risk of formation of reactive oxygen species by reaction with $^3P680$, both potentially leading to severe damage of the protein. A reduced yield of RP formation is therefore a protection mechanism. Even with this and other protection mechanisms, PS II becomes degraded and permanently has to be rebuilt as apparent from the rapid turnover of the D_1 protein (for a review see Andersson and Barber, 1996). On the other hand, double reduction of Q_A results in a high yield of RP formation. It probably occurs only under extreme conditions and might be a precursor state for photoinhibition and degradation of PS II (e.g., Vass et al., 1992).

A comparison of the RP yield in the different redox states of Q_A reveals the effect of electrostatic interactions within the RC protein. Due to a relatively low dielectric constant, the Coulomb interaction can amount to ~100 meV for a distance on the order of 15 Å. The change in the free energy is large enough to cause significant modifications of the electron transfer rates, except those that are kinetically optimized. This internal modulation of ΔG° gives, in principle, access to the reorganization energy in a way analogous to the application of an external electric field (Feher et al., 1988; Franzen et al., 1990; Dau et al., 1992) with the advantage that it is experimentally much easier to perform. Still another possibility to modify ΔG° would be to introduce in a controlled way charges in the protein by site-directed mutagenesis. This approach has been used successfully to modulate the midpoint potentials of cofactors and even the electron transfer pathways in RCs from purple bacteria (for a review see Woodbury and Allen, 1995).

APPENDIX 1

The analytical solutions for the time dependencies of the concentrations of the states B and C (Scheme 1) are, respectively

$$B(t) = [k_1\tau_1\tau_2/(\tau_2 - \tau_1)][-\exp(-t/\tau_1) + \exp(-t/\tau_2)] \quad \text{(A1)}$$

and

$$C(t) = [k_1k_2\tau_1\tau_2/(\tau_2 - \tau_1)] \cdot [\tau_1\exp(-t/\tau_1) - \tau_2\exp(-t/\tau_2) + \tau_2 - \tau_1], \quad \text{(A2)}$$

where τ_1 and τ_2 are functions of all molecular rate constants k_i (see below and Leibl et al., 1989). The photovoltage $PV(t)$ is the sum of the concentrations $B(t)$ and $C(t)$, weighted with their electrogenicity factors e_1 and e_2:

$$PV(t) = e_1B(t) + e_2C(t) \propto (1 + A_2^{app}) - \exp(-t/\tau_1) - A_2^{app}\exp(-t/\tau_2), \quad (A3)$$

where

$$A_2^{app} = [(e_2/e_1)k_2\tau_2 - 1]/[1 - k_2\tau_1(e_2/e_1)]. \quad (A4)$$

Note that $PV(t)$ contains only two exponential terms. Thus, it may also be expressed by only three apparent parameters, two exponential time constants τ_1 and τ_2 and one relative amplitude A_2^{app}, which can easily be determined by fitting the experimental traces.

Useful for calculations of molecular rate constants are the relations

$$(1/\tau_1) + (1/\tau_2) = k_1 + k_{-1} + k_2 + k_3 \quad (A5)$$

$$(1/\tau_1\tau_2) = k_{-1}k_3 + k_3k_2 + k_1k_2 \quad (A6)$$

and the expression for the maximum transient concentration of the RP, RP_{max}:

$$RP_{max} = [k_1/(1/\tau_1 - 1/\tau_2)][(\tau_2/\tau_1)^{[\tau_1/(\tau_1-\tau_2)]} - (\tau_2/\tau_1)^{[\tau_2/(\tau_1-\tau_2)]}]. \quad (A7)$$

The yield of charge stabilization, Y_{CS}, calculated as the concentration of the state C for open RCs at $t \to \infty$, $C(\infty)$, is given by the equation

$$Y_{CS} = k_1k_2/[k_1k_2 + k_3(k_2 + k_{-1})]. \quad (A8)$$

According to Scheme 1, the time dependence of the concentration of the excited state, $A(t)$ (and consequently of fluorescence) is given by

$$A(t) = a_1^{fl}\exp(-t/\tau_1) + a_2^{fl}\exp(-t/\tau_2), \quad (A9)$$

with the amplitude factors

$$a_1^{fl} = 1 - a_2^{fl} \quad (A10)$$

$$a_2^{fl} = [(k_2 + k_{-1}) - (1/\tau_2)]/[(1/\tau_1) - (1/\tau_2)]. \quad (A11)$$

The fluorescence yield, Φ^{fl}, is calculated as

$$\Phi^{fl} = \int_0^\infty A(t)dt = (k_2 + k_{-1})\tau_1\tau_2. \quad (A12)$$

APPENDIX 2

In the first approach (Table 3, sets 1 and 2) the input data for the calculations (Eqs. A4–A7) are the fit parameters of photovoltage traces and their relative peak amplitudes with the experimental errors of these quantities (Table 2). The only assumption made is that the value of k_3 is the same for all three redox states of Q_A. The relative electrogenicity of charge stabilization in the state Q_A, $e_2/e_1 = 1.85$ was taken from the literature (Leibl et al., 1989; Pokorny, 1994). Values of k_3 were fixed either to 1 ns^{-1} (set 1) or to 0.4 ns^{-1} (set 2). This range corresponds to the observed fluorescence lifetimes of isolated Chl antenna complexes and covers the range of values proposed for k_3 in the literature (Eads et al., 1987; Ide et al., 1987; Roelofs and Holzwarth, 1990; Roelofs et al., 1992; Mullineaux et al., 1993). It turns out that the value of k_3 has only a minor influence on the determination of the other molecular rate constants (for an extensive discussion see Roelofs and Holzwarth, 1990; see also Roelofs et al., 1992, Dau and Sauer, 1992).

In the second approach (Table 3, set 3) the input data for calculations (Eqs. A5–A7) are the time constants, τ, and the relative peak amplitudes of the photovoltage (Table 2). Additionally we applied some constraints, a part of them being based on fluorescence data. Besides trivial constraints (no negative rate constants, no negative fluorescence amplitudes) only the following very conservative constraints were used: 1) the yield of charge stabilization in open PS II, Y_{CS} (Eq. A8), is higher than 0.5 (Kramer and Mathis, 1980; Thielen and van Gorkom, 1981; Schatz et al., 1988); 2) the fluorescence yield, Φ^{fl} (Eq. A12), in the states Q_A^- and Q_AH_2 is at least twice as high as in the state Q_A (compare Table 1); 3) the fluorescence yield in the state Q_A^- is not lower than in the state Q_AH_2 (compare Table 1); 4) the amplitude of the slower fluorescence phase in the state Q_A, $a_2^{fl}(Q_A)$ (Eq. A11), is limited to the range $0.25 < a_2^{fl}(Q_A) < 0.7$ (compare $a_2(Q_A)$ in Table 1); 5) the rate of nonphotochemical decay of the excited state, k_3, is the same in both reduced states of Q_A; and 6) this rate is not higher than in open RCs ($k_3(Q_A) \geq k_3(Q_A^-) = k_3(Q_AH_2)$). The assumption that $k_3(Q_A^-) = k_3(Q_AH_2)$ is probably justified because the redox potential was the same in both samples, excluding, e.g., different quenching power of the plastoquinone pool. On the other hand, the conditions $k_3(Q_A) \geq k_3(Q_A^-)$ and $k_3(Q_A) \geq k_3(Q_AH_2)$ account for a possible quenching of excited states by the oxidized plastoquinone pool (Delosme, 1967; Vernotte et al., 1979; Pokorny, 1994). In this second approach we use an iteration procedure to narrow down the ranges of possible values for the molecular rate constants.

Financial support by the French-Polish Joint Project (Projet Concerté de Coopération Scientifique 5325, 6325, and 7325) is acknowledged. K.G. was supported by a fellowship of the French Government.

REFERENCES

Andersson, B., and J. Barber. 1996. Mechanisms of photodamage and protein degradation during photoinhibition of photosystem II. *In* Advances in Photosynthesis: Photosynthesis and the Environment. N. R. Baker, editor. Kluwer Academic Publishers, Dordrecht, The Netherlands. 101–121.

Berthold, D. A., G. T. Babcock, and C. F. Yocum. 1981. A highly resolved, oxygen-evolving photosystem II preparation from spinach thylakoid membranes: EPR and electron-transport properties. *FEBS Lett.* 134: 231–234.

Booth, P. J., B. Crystall, I. Ahmad, J. Barber, G. Porter, and D. R. Klug. 1991. Observation of multiple radical pair states in photosystem 2 reaction centers. *Biochemistry.* 30:7573–7586.

Chang, H. C., R. Jankowiak, N. R. S. Reddy, C. F. Yocum, R. Picorel, M. Seibert, and G. J. Small. 1994. On the question of the chlorophyll a content of the photosystem II reaction center. *J. Phys. Chem.* 98: 7725–7735.

Dau, H., and K. Sauer. 1992. Electric field effect on the picosecond fluorescence of photosystem II and its relation to the energetics and kinetics of primary charge separation. *Biochim. Biophys. Acta.* 1102: 91–106.

Delosme, R. 1967. Etude de l'induction de fluorescence des algues et des chloroplastes au début d'une illumination intense. *Biochim. Biophys. Acta.* 143:108–128.

Diner, B. A., and G. T. Babcock. 1996. Structure, dynamics, and energy conversion efficiency in photosystem II. *In* Advances in Photosynthesis. Oxygenic Photosynthesis: The Light Reactions. D. R. Ort and C. F. Yocum, editors. Kluwer Academic Publishers, Dordrecht, The Netherlands. 213–247.

Eads, D. D., S. P. Webb, T. G. Owens, L. Mets, R. S. Alberte, and G. R. Fleming. 1987. Characterization of the fluorescence decays of the chlorophyll a/b protein. *In* Progress in Photosynthesis Research, Vol. 1. J. Biggins, editor. Nijhoff, Dordrecht, The Netherlands. 135–138.

Feher, G., T. R. Arno, and M. Y. Okamura. 1988. The effect of an electric field on the charge recombination rate of $D^+Q_A^- \rightarrow DQ_A$ in reaction centers from *Rhodobacter sphaeroides* R-26. *In* The Photosynthetic Bacterial Reaction Center; Structure and Dynamics. J. Breton, and A. Verméglio, editors. Plenum Press, New York. 271–287.

Franzen, S., R. F. Goldstein, and S. G. Boxer. 1990. Electric field modulation of electron transfer rates in isotropic systems: long-distance charge recombination in photosynthetic reaction centers. *J. Phys. Chem.* 94:5135–5149.

Geacintov, N. E., and J. Breton. 1987. Energy transfer and fluorescence mechanisms in photosynthetic membranes. *CRC Crit. Rev. Plant Sci.* 5:1–44.

Greenfield, S. R., M. Seibert, Govindjee, and M. R. Wasielewski. 1997. Direct measurement of the effective rate constant for primary charge separation in isolated photosystem II reaction centers. *J. Phys. Chem. B.* 101:2251–2255.

Guenther, J. E., and A. Melis. 1990. The physiological significance of photosystem II heterogeneity in chloroplasts. *Photosynth. Res.* 23: 105–109.

Hansson, Ö., J. Duranton, and P. Mathis. 1988. Yield and lifetime of the primary radical pair in preparations of photosystem II with different antenna size. *Biochim. Biophys. Acta.* 932:91–96.

Hodges, M., and I. Moya. 1986. Time-resolved chlorophyll fluorescence studies of photosynthetic membranes: resolution and characterization of four kinetic components. *Biochim. Biophys. Acta.* 849:193–202.

Holzapfel, W., U. Finkele, W. Kaiser, D. Oesterhelt, H. Scheer, H. U. Stilz, and W. Zinth. 1989. Observation of a bacteriochlorophyll anion radical during the primary charge separation in a reaction center. *Chem. Phys. Lett.* 160:1–7.

Holzapfel, W., U. Finkele, W. Kaiser, D. Oesterhelt, H. Scheer, H. U. Stilz, and W. Zinth. 1990. Initial electron-transfer in the reaction center from *Rhodobacter sphaeroides. Proc. Natl. Acad. Sci. U.S.A.* 87:5168–5172.

Holzwarth, A. R. 1991. Excited-state kinetics in chlorophyll systems and its relationship to the functional organization of the photosystems. *In* Chlorophylls: CRC Handbook. H. Scheer, editor. CRC Press, Boca Raton, FL. 1125–1151.

Holzwarth, A. R., and M. G. Müller. 1996. Energetics and kinetics of radical pairs in reaction centers from *Rhodobacter sphaeroides*: a femtosecond transient absorption study. *Biochemistry.* 35:11820–11831.

Ide, J. P., D. R. Klug, W. Kühlbrandt, L. B. Giorgi, and G. Porter. 1987. The state of detergent solubilised light-harvesting chlorophyll-*a*/*b* protein complex as monitored by picosecond time-resolved fluorescence and circular dichroism. *Biochim. Biophys. Acta.* 893:349–364.

Kramer, H., and P. Mathis. 1980. Quantum yield and rate of formation of the carotenoid triplet state in photosynthetic structures. *Biochim. Biophys. Acta.* 593:319–329.

Krishtalik, L. I. 1989. Activationless electron transfer in the reaction centre of photosynthesis. *Biochim. Biophys. Acta.* 977:200–206.

Leibl, W., J. Breton, J. Deprez, and H.-W. Trissl. 1989. Photoelectric study on the kinetics of trapping and charge stabilization in oriented PS II membranes. *Photosynth. Res.* 22:257–275.

Liu, B., A. Napiwotzki, H.-J. Eckert, H. J. Eichler, and G. Renger. 1993. Studies on the recombination kinetics of the radical pair $P680^+Pheo^-$ in isolated PS II core complexes from spinach. *Biochim. Biophys. Acta.* 1142:129–138.

Marcus, R. A. 1956. On the theory of oxidation-reduction reactions involving electron transfer. *J. Chem. Phys.* 24:966–978.

Marcus, R. A., and N. Sutin. 1985. Electron transfers in chemistry and biology. *Biochim. Biophys. Acta.* 811:265–322.

McCauley, S. W., E. Bittersmann, and A. R. Holzwarth. 1989. Time-resolved ultrafast blue-shifted fluorescence from pea chloroplasts. *FEBS Lett.* 249:285–288.

Müller, M. G., M. Hucke, M. Reus, and A. R. Holzwarth. 1996. Primary processes and structure of the photosystem II reaction center. IV. Low intensity femtosecond transient absorption spectra of D1–D2-cyt-b559 reaction centers. *J. Phys. Chem.* 100:9527–9536.

Mullineaux, C. W., A. A. Pascal, P. Horton, and A. R. Holzwarth. 1993. Excitation-energy quenching in aggregates of the LHC II chlorophyll-protein complex: a time-resolved fluorescence study. *Biochim. Biophys. Acta.* 1141:23–28.

Nuijs, A. M., H. J. van Gorkom, J. J. Plijter, and L. N. M. Duysens. 1986. Primary-charge separation and excitation of chlorophyll *a* in photosystem II particles from spinach as studied by picosecond absorbance-difference spectroscopy. *Biochim. Biophys. Acta.* 848:167–175.

Peloquin, J. M., J. C. Williams, X. Lin, R. G. Alden, A. K. W. Taguchi, J. P. Allen, and N. W. Woodbury. 1994. Time-dependent thermodynamics during early electron transfer in reaction centers from *Rhodobacter sphaeroides. Biochemistry.* 33:8089–8100.

Pokorny, A. 1994. Kinetische und strukturelle Aspekte von Photosystem II. Ph.D. Thesis. Universität Osnabrück, Osnabrück, Germany. 31–110.

Roelofs, T. A., M. Gilbert, V. A. Shuvalov, and A. R. Holzwarth. 1991. Picosecond fluorescence kinetics of the D_1-D_2-Cyt *b*-559 photosystem II reaction center complex: energy transfer and primary charge separation processes. *Biochim. Biophys. Acta.* 1060:237–244.

Roelofs, T. A., and A. R. Holzwarth. 1990. In search of a putative long-lived relaxed radical pair state in closed photosystem II: kinetic modeling of picosecond fluorescence data. *Biophys. J.* 57:1141–1153.

Roelofs, T. A., C.-H. Lee, and A. R. Holzwarth. 1992. Global target analysis of picosecond chlorophyll fluorescence kinetics from pea chloroplasts: a new approach to the characterization of the primary processes in photosystem II α- and β-units. *Biophys. J.* 61:1147–1163.

Rutherford, A. W., and W. Nitschke. 1996. Photosystem II and the quinone-iron-containing reaction centers: comparisons and evolutionary perspectives. *In* Origin and Evolution of Biological Energy Conversion. H. Baltscheffsky, editor. VCH Publishers, New York.177–203.

Schatz, G. H., H. Brock, and A. R. Holzwarth. 1987. Picosecond kinetics of fluorescence and absorbance changes in photosystem II particles excited at low photon density. *Proc. Natl. Acad. Sci. U.S.A.* 84: 8414–8418.

Schatz, G. H., H. Brock, and A. R. Holzwarth. 1988. Kinetic and energetic model for the primary processes in photosystem II. *Biophys. J.* 54: 397–405.

Schelvis, J. P. M., P. I. van Noort, T. J. Aartsma, and H. J. van Gorkom. 1994. Energy transfer, charge separation and pigment arrangement in the reaction center of photosystem II. *Biochim. Biophys. Acta.* 1184: 242–250.

Schlodder, E., and K. Brettel. 1988. Primary charge separation in closed photosystem II with a lifetime of 11 ns: flash-absorption spectroscopy with O_2-evolving photosystem II complexes from *Synechococcus. Biochim. Biophys. Acta.* 933:22–34.

Sundby, C., A. Melis, P. Mäenpää, and B. Andersson. 1986. Temperature-dependent changes in the antenna size of photosystem II: reversible conversion of photosystem II_α to photosystem II_β. *Biochim. Biophys. Acta.* 851:475–483.

Takahashi, Y., Ö. Hansson, P. Mathis, and K. Satoh. 1987. Primary radical pair in the photosystem II reaction center. *Biochim. Biophys. Acta.* 893:49–59.

Thielen, A. P. G. M., and H. J. van Gorkom. 1981. Energy transfer and quantum yield in photosystem II. *Biochim. Biophys. Acta.* 637:439–446.

Trissl, H.-W. 1993. Long-wavelength absorbing antenna pigments and heterogeneous absorption bands concentrate excitons and increase absorption cross section. *Photosynth. Res.* 35:247–263.

Trissl, H.-W., and K. Wulf. 1995. Fast photovoltage measurements in photosynthesis. II. Experimental methods. *Biospectroscopy.* 1:71–82.

van Gorkom, H. J. 1985. Electron transfer in PS II. *Photosynth. Res.* 6:97–112.

van Mieghem, F. J. E. 1994. Photochemistry and structural aspects of the photosystem II reaction centre. Ph.D. Thesis. Landbouw Universiteit Wageningen, Wageningen, The Netherlands. 1–35.

van Mieghem, F. J. E., K. Brettel, B. Hillmann, A. Kamlowski, A. W. Rutherford, and E. Schlodder. 1995. Charge recombination reactions in photosystem II. I. Yields, recombination pathways, and kinetics of the primary pair. *Biochemistry.* 34:4798–4813.

van Mieghem, F. J. E., G. F. W. Searle, A. W. Rutherford, and T. J. Schaafsma. 1992. The influence of the double reduction of Q_A on the

fluorescence decay kinetics of photosystem II. *Biochim. Biophys. Acta.* 1100:198–206.

Vass, I., G. Gatzen, and A. R. Holzwarth. 1993. Picosecond time-resolved fluorescence studies on photoinhibition and double reduction of Q_A in Photosystem II. *Biochim. Biophys. Acta.* 1183:388–396.

Vass, I., S. Styring, T. Hundal, A. Koivuniemi, E.-M. Aro, and B. Andersson. 1992. Reversible and irreversible intermediates during photoinhibition of photosystem II: stable reduced Q_A species promote chlorophyll triplet formation. *Proc. Natl. Acad. Sci. U.S.A.* 89:1408–1412.

Vernotte, C., A.-L. Etienne, and J. M. Briantais. 1979. Quenching of the system II chlorophyll fluorescence by the plastoquinone pool. *Biochim. Biophys. Acta.* 545:519–527.

Wasielewski, M. R., D. G. Johnson, M. Seibert, and Govindjee. 1989. Determination of the primary charge separation rate in isolated photosystem II reaction centers with 500-fs time resolution. *Proc. Natl. Acad. Sci. U.S.A.* 86:524–528.

Woodbury, N. W., and J. P. Allen. 1995. The pathway, kinetics and thermodynamics of electron transfer in wild type and mutant reaction centers of purple nonsulfur bacteria. *In* Advances in Photosynthesis: Anoxygenic Photosynthetic Bacteria. R. E. Blankenship, M. T. Madigan, and C. E. Bauer, editors. Kluwer Academic Publishers, Dordrecht, The Netherlands. 527–557.

Woodbury, N. W., and W. W. Parson. 1984. Nanosecond fluorescence from isolated photosynthetic reaction centers of *Rhodopseudomonas sphaeroides. Biochim. Biophys. Acta.* 767:345–361.

Wulf, K., and H.-W. Trissl. 1995. Fast photovoltage measurements in photosynthesis. I. Theory and data evaluation. *Biospectroscopy.* 1:55–69.

Yruela, I., G. Gatzen, R. Picorel, and A. R. Holzwarth. 1996. Cu(II)-inhibitory effect on photosystem II from higher plants: a picosecond time-resolved fluorescence study. *Biochemistry.* 35:9469–9474.